CHEMISTRY
A EUROPEAN JOURNAL

DOI: 10.1002/chem.200800445

A Structure-Consistent Mechanism for Dioxygen Formation in Photosystem II

Per E. M. Siegbahn*[a]

Abstract: In recent DFT studies a new mechanism for O–O bond formation at the oxygen evolving center (OEC) in photosystem II has been suggested. With the structure of the S_4 state required for that mechanism, the structures of the lower S states are investigated herein by adding protons and electrons. A model was used including the full amino acids for the ones ligating the OEC, and in which the backbone positions were held fixed from the X-ray structure. The only charged second-shell ligand Arg357 was also included. An optimized structure for the S_1 state was reached with a large similarity to one of those suggested by EXAFS. A full catalytic cycle was derived which can rationalize the structural relaxation in the S_2 to S_3 transition, and the fact that only an electron leaves in the transition before. Water is suggested to bind to the OEC in the S_2 to S_3, and S_4 to S_0 transitions. A new possibility for water exchange is suggested from the final energy diagram. The optimal O–O bond formation occurs between an oxygen radical and an oxo ligand. The alternative mechanism, where the oxygen radical reacts with an external water, has a barrier about 20 kcal mol^{-1} higher.

Keywords: density functional calculations · manganese · oxygen · photosystem

Introduction

Photosystem II is the only system in nature capable of forming dioxygen from water and sunlight. The catalyst for the step where the O–O bond is formed is the oxygen evolving complex (OEC) located close to the lumenal side in the membrane. Briefly, dioxygen is formed after oxidizing the OEC in four steps, passing so called S states from S_0 to S_4. In each S state transition protons may also be lost, in total removing four electrons and four protons from two water molecules, leaving the oxygen atoms to form O_2. The OEC complex contains four manganese and one calcium atom. Recent X-ray diffraction studies have considerably clarified the detailed structure of the OEC.[1,2] In the first of these recent studies,[1] it was shown that three of the manganese and the calcium atom forms a cuboidal structure with the fourth manganese situated outside the cube. The amino acids most likely to be ligated to the complex were also assigned, see Figure 1. Since the resolution was rather low (3.5 Å), the exact ligation pattern could only be suggested. Most of the amino acid ligands were assigned as binding to one manganese each, mono- or bidentately. Based on EXAFS measurements,[3] the metal atoms were assumed to be connected by μ-oxo bonds. The remaining coordination sites would then have to be occupied by water derived ligands. In the most recent X-ray structure the resolution was slightly higher (3.0 Å),[2] and a different ligation pattern was suggested. Most of the carboxylate amino acid ligands were now assumed to bind bidentately between two different

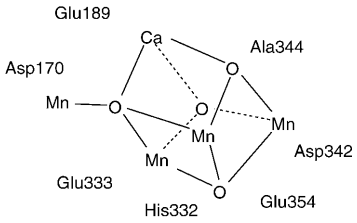

Figure 1. Simplified picture of the structure of the oxygen evolving complex, suggested by X-ray crystallography.

[a] Prof. Dr. P. E. M. Siegbahn
Department of Physics
ALBA NOVA and Department of Biochemistry and Biophysics
Arrhenius Laboratory, Stockholm University
10691 Stockholm (Sweden)
Fax: (+46) 855378601
E-mail: ps@physto.se

Supporting information for this article is available on the WWW under http://dx.doi.org/10.1002/chem.200800445: The structures of all the states in the diagram in Figure 14.

metal atoms. This means that hardly any water derived ligands had to be added to saturate the metal coordination sites. The positions of the metal atoms were similar to the ones in the earlier X-ray structure, with the exception that the dangling manganese was placed farther out from the Mn_3Ca cube. These two X-ray structures will in the following be termed the London and the Berlin structures. The expression dangling manganese will be used in the present paper only to specify that this manganese is outside the Mn_3Ca cube, but not the character of the bonding between this maganese and the cube. In some structures discussed below, the dangling manganese will in fact be quite strongly bound to the cube.

Parallel to the experimental structural work, significant progress has been made on the mechanism for O–O bond formation by using density functional theory (DFT). Prior to the first X-ray structures, the main result of those studies was that the O–O bond formation appeared to require the initial formation of an oxygen radical bound to manganese. The O–O bond was then suggested to be formed between the oxygen radical and an external water molecule.[4,5] After the X-ray structures appeared, more detailed mechanistic studies could be performed. Following those studies the same type of O–O bond formation remained most likely.[6–8] The studies furthermore indicated that the bicarbonate ligand suggested by the X-ray analysis is an unlikely ligand.

In the theoretical studies mentioned above, a few other important steps were taken towards a more detailed picture of the oxygen evolving process. For example, a new approach was designed to construct a reliable energy diagram for the full reaction cycle. Absolute redox potentials and pK_a values, required for the energy diagram, are known to be difficult to obtain accurately enough by models of limited size. However, relative values should be much more reliable. Using only these relative values and some key experimental information, an accurate diagram should be obtainable, provided that the closest surrounding of the active site does not change from one transition to another.[7–13]

At the stage of the above-mentioned studies, the preferred mechanism for O–O bond formation was always an attack on the oxygen radical by an external water. However, if the oxygen radical was not produced exergonically (or thermo-neutrally), the computed barrier for this mechanism was far too high. A scenario where the oxygen radical was easily obtained was never found. Instead, this step was always found to be endergonic by at least 10 kcal mol^{-1}. In order to obtain progress, a different approach was adopted, where the lowest energy oxygen radical state of the OEC was investigated in detail. Essentially all possible pathways to form the O–O bond were investigated and the result was very surprising. A quite low barrier was found when the oxygen radical formed the bond to an oxo ligand in the cube.[14] There are also additional spin requirements on this mechanism, where the atoms involved in the bond formation, the two oxygen atoms and two manganese, have alternating spins. This mechanism has recently been reviewed.[15,16]

The O–O bond formation mechanism mentioned above is strongly preferred in all calculations done to date, so that it actually must be considered the most certain theoretical result obtained in the entire catalytic cycle. In the present study, this mechanism was again compared with the leading alternatives and found to be far superior. However, the structures obtained in the previous studies are less satisfactory. The strategy, based on previous experience, was to assume that the main features of the mechanism would be rather insensitive to the details of the structures. In the present study, the goal is instead to obtain improved structures for the different S states. The starting point is the oxygen radical S_4 state. A structure, better in line with experimental structural information, is obtained by fixing the positions of the backbone atoms of the amino acid ligands of the OEC from the London structure. Only ligands suggested to bind to the OEC were retained in the model, plus one additional amino acid, Arg357, since it is the closest amino acid that is charged. Structures of the lower S states were then obtained from the S_4 state by adding electrons and protons to the OEC, that is, going backwards in the catalytic cycle. At two stages, water molecules had to be removed. The results are compared to the experimentally suggested structures and results obtained by spectroscopic investigations.

So far, there has been essentially only one other computational attempt to find the mechanism of dioxygen formation in PSII.[17] In that approach, a large portion of the protein was incorporated into the model using the QM/MM method. The London X-ray structure was used as a starting point for the geometry optimizations. The analysis was focused on one type of mechanism suggested earlier based on experiments,[18] where a water bound to calcium attacks a Mn^V–oxo group. QM/MM is a much more cumbersome approach than the one used in the present study, and for this reason no redox potentials, pK_a values or transition states were computed. General arguments, rather than the energies obtained from the QM/MM approach were used to test if the mechanism was plausible. The results support the mechanism investigated, with the modification that the Mn^V–oxo was found to be a Mn^{IV}–oxyl state, and the water bound to calcium was better represented as an external water, both findings in line with the old mechanism found in the earlier studies mentioned above.[4–8]

Results and Discussion

Methods and models

The calculations discussed here were made by using the DFT hybrid functional B3LYP,[19] with procedures rather similar to those used in previous studies.[6–8,14–16] The performance of the B3LYP functional for the present type of problems has recently been reviewed,[20] indicating a typical accuracy of 3–5 kcal mol^{-1}, normally overestimating barriers. One difference between the present and earlier studies is that the geometries have been optimized with a polarized

basis set (lacvp*), whereas an unpolarized basis set (lacvp) was used earlier. The final relative energies are quite insensitive to this extension, but some of the metal–metal distances become notably better compared to EXAFS experiments. The geometries of stable points were fully optimized only with the constraint of some frozen atomic positions taken from the X-ray structure (see further below). Since Hessians could not be computed for the present large models, the transition states were instead obtained with two critical distances frozen from earlier optimizations on smaller models. These distances are the O–O bond and one of the Mn–O bonds directly involved. The potential surface around the TS is very flat and the computed barrier should be quite insensitive to this approximation. In the optimized geometries, single point calculations were performed using a large basis set, cc-pvtz(-f) for first row atoms and lacv3p+ for the metals. In one case, the oxygen radical S_4 state, the energy needed to be corrected for spin contamination using a standard procedure.[21] The correction lowers the S_4 state energy by 2.6 kcal mol^{-1}.

A significant difference compared with the previous studies is that the final energies were obtained with a modification of the standard B3LYP functional. Instead of a 20% fraction exact exchange, 15% was used (termed B3LYP*).[22] This has been shown to be an improvement in nearly all transition metal containing systems tested so far.[20] For molecules without transition metals the slight reduction of exact exchange has almost no effect. In the present calculations the most important effect is a decrease of the redox potential going from Mn^{III} to Mn^{IV} by about 5 kcal mol^{-1} (0.2 V). Since only relative redox potentials are used in practice in the present approach, see further below, this has only two effects in the energy diagram. First, the binding of O_2 becomes about 10 kcal mol^{-1} stronger, and secondly, the difference between the redox-potential of manganese (Mn^{III} to Mn^{IV}) and oxygen (going to an oxygen radical) changes by 5 kcal mol^{-1}.

Zero-point vibrational effects have been taken from earlier calculations on smaller models. For a proton release there is a loss of 7–9 kcal mol^{-1}, while for electron release there is a small gain of 1–2 kcal mol^{-1}. Again, for the relative redox potentials and pK_a values, the inclusion of zero-point has only very small effects. From experience, entropy effects are of little importance except for the step where O_2 is released, where entropy increases by about 10 kcal mol^{-1}. Compared with the earlier studies, where standard B3LYP (20% exact exchange) was used and entropy was neglected, the binding energy of dioxygen is therefore not significantly changed, since going to 15% exchange increases the binding by 10 kcal mol^{-1} (see above). This cancellation, which has been an empirical finding in many studies,[20] was deliberately used in the previous studies.

As in previous studies, surrounding polarization of the protein medium was described by a dielectric cavity approach. A dielectric constant of 4.0 was employed as usual, and the probe radius was chosen as 1.40 Å. Absolute values of both redox potentials and pK_a values are quite sensitive to the choice of dielectric constant, but since only relative values are needed in the diagram, the effect of varying the dielectric constant is very small. For example, the effect of using $\varepsilon = 8$ can be estimated from the formula,

$$E = (\varepsilon - 1)/\varepsilon q^2/2R$$

which means that they are obtained from the ones with $\varepsilon =$ 4, by scaling them with a factor of 7/6. In the diagram discussed below (see Figure 14, where $\varepsilon = 4$ was used), the effects on the 12 energy levels will then be: 0.0, +0.6, −0.1, −0.5, −0.3, 0.0, +0.3, +0.4, +0.1, +0.1, +0.5, and 0.0 kcal mol^{-1}. In fact, even neglecting the dielectric effects would not severely affect the diagrams. The dielectric effects were computed with a polarized triple zeta basis set (lacv3p*), which is somewhat larger than the basis set used earlier (lacvp*). No significant effect is expected due to this extension.

As already indicated, a different procedure than used by other workers for obtaining redox potentials and pK_a values is a key feature of the present approach.[7–13] For the energy diagrams only relative redox and pK_a values are used. To relate the calculated relative values to the actual situation in the enzyme, both experimental information about the driving force, and a single adjustable parameter are used as described in detail in earlier work. Thus it is possible to determine accurate energy diagrams without explicitly describing the enzyme surrounding the active site. The calculations were performed with the Jaguar program.[23]

The chemical model used in most of the calculations is shown in Figure 2. The decision made at the onset of the optimizations was to follow the suggestions from the most recent X-ray study[2] and use a ligation where most carboxylic groups are bidentately bound to two metals. This is a very common binding type in metalloenzymes and has the attractive feature that almost the full coordination of the OEC is controlled by the amino acids. Only two water derived ligands (placed on the dangling manganese) are needed to fill up all the coordination sites of manganese. Two water molecules were also placed on calcium. To stay as close as possible to the X-ray density some atoms were held fixed at their suggested positions in the X-ray structure. It was decided that the backbone atoms are the ones that were most accurately positioned in the X-ray structure and these were therefore held fixed. The choice was made to take these positions from the London structure. Since the cut of each amino acid model is at the α-carbon, this atom was replaced by a methyl group where one carbon and two hydrogens (those along the backbone) were held fixed. The exception is His332-Glu333 where the full backbone between them was kept. In this case only the α-carbons were held fixed. There are very many local minima for the amino acid positions, and the optimization was therefore manually guided towards the desired ligand coordination, the one of the Berlin structure. It can therefore not be concluded that the final structure should be in an absolute minimum, but could

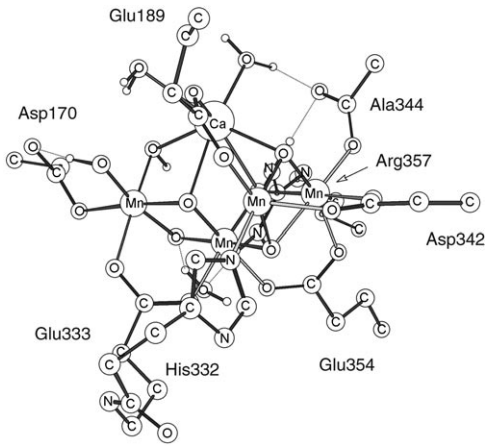

Figure 2. Fully optimized structure for the lowest energy S_1^{-2} state. Most of the amino acid protons have been removed for a better visualization.

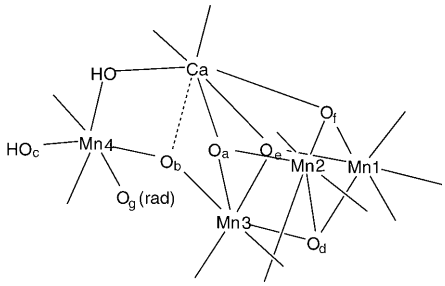

Figure 3. Simplified picture of the S_4^{-1} state, which represents the starting point for the optimizations. All manganese are Mn^{IV}.

also be in only a local minimum. The accuracy of the final structure has to be based on comparisons to available experimental results such as to EXAFS.

Structures and mechanism

Starting point: The results of the present study will be presented both in chronological and mechanistic order. It is important to realize that the starting point for the present investigation is the oxygen radical S_4 state, which is the state where the O–O bond is formed. A simplified picture is shown in Figure 3, where the O–O bond is formed between O_g(rad) and O_a. The nomenclature for the S states is the same as in earlier papers, with a lower index indicating the S-state number, and the upper index the charge of the OEC complex not counting groups that are not directly bound to the metals. The state in the figure is then labeled S_4^{-1}. The mechanism for the step where the O–O bond is formed is considered to be the most reliable information obtained from the previous theoretical investigations, and the S_4 state therefore represents the best possible starting point for a structural investigation. This conclusion is drawn since all other mechanisms investigated have very much higher barriers. In contrast, if a structure for a lower S state should be chosen as starting point, the calculations have shown that there are many more candidates to choose from. For example, the choice of protonating different oxo ligands, or choosing which manganese that is Mn^{III} or Mn^{IV}, leads to many possibilities. For S_4, the oxo bridges should not be protonated and all manganese should be Mn^{IV}.

There are a few particularly important features of the S_4 structure that are required for a low barrier for O–O bond formation. The main requirements are that the oxygen radical (O_g(rad)) is held by the dangling manganese (Mn4) and that the oxo group (O_a) is within reach. For optimal overlap, the dangling manganese has to be at a sufficiently long distance from the cube. For example, the position given in the London structure would not suffice, since Mn4 is actually bound directly to O_a. On the other hand, the position given in the Berlin structure would fit well. It is also required that the oxo group is held by many metal bonds, which in practice leads to a fully formed cube between three manganese and calcium. At the stage of O–O bond formation the number of easily removable protons should furthermore be minimized, suggesting that no oxo ligand bridging the manganese atoms should be protonated and the terminal water derived ligand on Mn4 should be a hydroxyl group.

Reaching an S_1 structure: From the above S_4 state, the S_1 state can be reached by adding electrons and protons. It is important to obtain a suggestion for the structure of the S_1 state, since this is the resting state for which the experimental information is most abundant. In the calculations the S_1 state is reached from the S_4 state by adding protons to different oxygens, and reducing the different metals in all possible ways, always searching for the state with the lowest energy. It is also important to check whether any water molecule should be removed. The rule of thumb is that if the binding enthalpy to the OEC is smaller than 14 kcal mol^{-1}, the water molecule would be better bound in the water bulk than to the complex.

How the S_1 state was reached from the S_4 state will be briefly described here. The sequence going the opposite way, from the beginning to the end in the catalytic cycle, will be described more in detail below. The first electron to be added to S_4 is obviously to the oxygen radical. The first proton must then be added to the same oxygen, since a terminal Mn–oxo group is never favorable. There is no possibility for O_g to bind to Mn3 since this metal is already six-coordinated. The S_3 state has now been reached.

An interesting structural change occurs when the next electron and proton are added. The best place to add an electron turns out to be to Mn2, which now has oxidation state III, and the best place for a proton is at O_g, which has now become a water molecule. When this water molecule is removed, Mn4 completes its six-coordination by forming a bond to O_a. In this process, the bond between Mn2 and O_a is lost, leading to a five-coordinated Mn2, which is preferable since it now has oxidation state III (see further below). The Jahn–Teller axis is formed in the direction of the empty coordination site as usual. All these structural changes occurred automatically in some of the geometry optimizations.

In others, the structure was trapped in a local minimum, one of them with O_a forming a bond to both Mn2 and Mn4. However, the lowest energy minimum was found for the structure described above. In the detailed investigations, it was found that instead adding a proton on the OH-group bridging the dangling manganese and calcium, led to the same structure for the S_2 state after some rearrangements. A structural change of the type described here in the S_2 to S_3 transition has been suggested before from the results in some of the previous DFT studies.[14] A general structural change in this transition has also been suggested experimentally mainly from EXAFS investigations,[25,26] but the type of suggested structural change has varied between the different studies. It is interesting to note that in one of those studies[26] a structural change was suggested involving Mn2 becoming six-coordinated, like in the present suggestion, but without involvement of any external water.

The S_2 state reached in the process described above has a much shorter distance between the dangling manganese Mn4 and the Mn_3Ca cube, than the one of the S_4 starting structure in Figure 3. The energy of this compact structure can be compared with the more open S_2 structure, that would have been reached from the S_3 structure if the water molecule had stayed on the OEC and not been removed and placed in bulk water (binding energy 14 kcal mol^{-1}). This state was found to be as much as 12 kcal mol^{-1} higher in energy, showing that, indeed, the lowest energy S_2 state is more compact than the starting S_4-type structure.

The S_1 state is reached from the S_2 state by adding yet another electron. The best structure obtained is shown in Figure 2, and in simplified versions in Figure 4. One of the most interesting features of this structure is the binding between the dangling manganese Mn4 to Mn3 in the Mn_3Ca cube, with two μ-oxo bonds rather than only one. This particular feature is not present in any of the X-ray structures but has been suggested by most EXAFS studies.[28,29] A characteristic new feature of the S_1 structure in Figure 4 is that the Mn_3Ca cube is not complete, since the bond between Mn2 and O_a is missing.

The optimized S_1^{-2} structure is placed in the X-ray density from the London study in Figure 5. This can be easily done since all backbone atoms were held fixed from the London structure in the optimization. As seen in the figure, the structure fits very well into the density. Two conclusions can be drawn. First, the structure obtained in the DFT optimization is at least an equally valid candidate for the correct structure as those suggested in the X-ray analysis. Second, there is no indication from this figure that the density obtained in the London experiment has suffered in a major way from X-ray damage. There need not be any contradiction between this conclusion and the results from an EXAFS investigation,[30] showing that all short Mn–Mn distance are lost at high X-ray doses. To be more precise, changes of the Mn distances by 0.3–0.4 Å may not change the overall density very much. On the other hand, changes on the order of 1.0 Å would have changed the density and should have been noticeable in Figure 5.

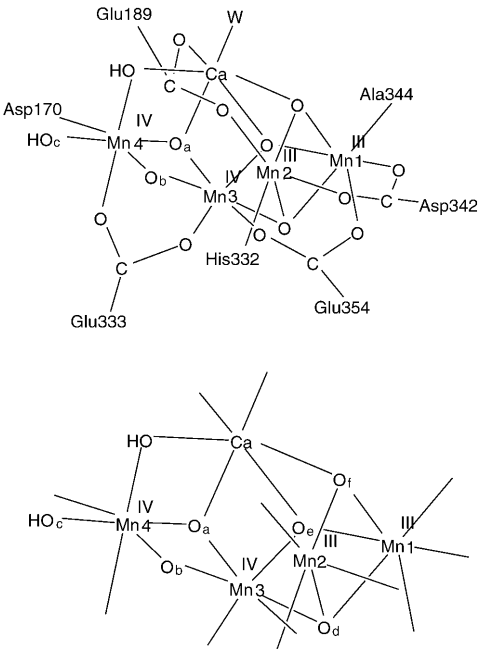

Figure 4. Simplified pictures of the S_1^{-2} state.

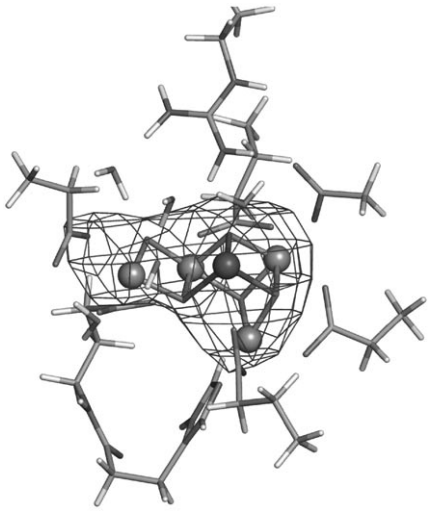

Figure 5. DFT optimized S_1^{-2} structure placed into the X-ray density from the London X-ray measurements.

A comparison of the DFT optimized structure of the OEC with the one from the London X-ray analysis is shown in Figure 6. Since the DFT optimization was done with some backbone atoms held fixed from the London X-ray structure,[1] the relative orientation of the two structures is given automatically. Even though there are general similarities between the structures, there are also some clear differences in the positioning of the atoms, as shown in the figure. The distances between the corresponding atoms are for **1L** and **1** 1.5 Å, for **2L** and **2** 1.4 Å, for **3L** and **3** 0.9 Å, for **4L** and **4** 0.6 Å, and for about 0.9 Å. It should be added, as mentioned above, that both structures fit the X-ray density well, perhaps slightly better for the DFT structure.

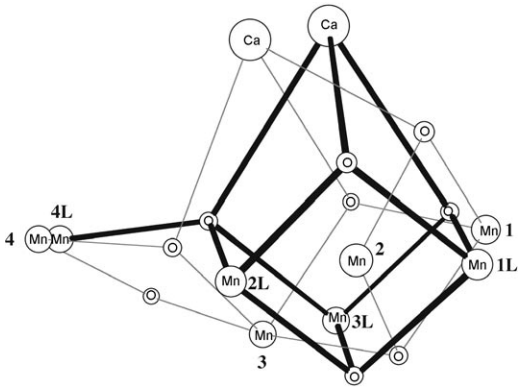

Figure 6. DFT structure superimposed on the London X-ray structure. The X-ray atoms are marked with an **L** and are connected by thick lines, the DFT atoms with a thin line.

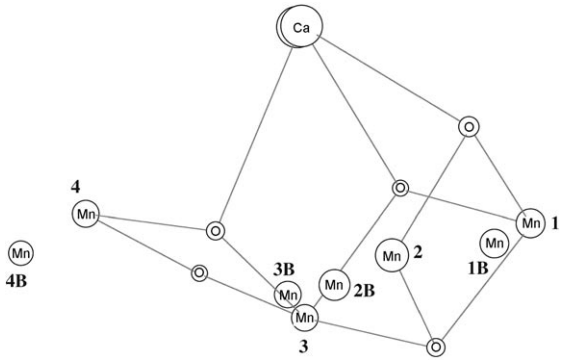

Figure 7. DFT structure superimposed on the Berlin X-ray structure. The X-ray atoms are marked with a **B**. The DFT atoms are connected with a thin line.

A corresponding comparison between the DFT structure and the one obtained from the Berlin X-ray analysis[2] is shown in Figure 7. In this case the X-ray atoms could not be connected since no positions for the oxygen atoms were suggested. The relative orientation of the DFT and the Berlin structures was obtained by first orienting the Berlin structure to the London structure, which could be made from the corresponding PDB-files by placing three backbone atoms as close to each other as possible. Again, there is a general similarity between the DFT and the Berlin structure but the detailed positions are different. The distance between **1B** and **1** is 0.6 Å, between **2B** and **2** 0.6 Å, between **3B** and **3** 0.6 Å, between **4B** and **4** 1.8 Å, and for the two Ca only 0.1 Å. The DFT position of the dangling manganese Mn4 is worth noting. This atom is much closer to its position in the London structure, 0.6 Å, compared to 1.8 Å in the Berlin structure. On the other hand, the DFT position of manganese atom **2** is closer to its position in the Berlin structure than in the London structure, 0.6 Å compared to 1.4 Å. It should be added that the positions obtained for the metal atoms in the DFT optimization depends to some extent on the choice of atoms that were held fixed from the X-ray structure. Most of the positions frozen (all in the backbone) are very similar in the two X-ray structures, except for Asp170 and Ala344. Choosing to fix the positions of these amino acid backbones from the Berlin structure instead could lead to a position further out for Mn4 in the DFT optimization.

A similar comparison can also be made between the present DFT structure and the four different explicit structures suggested by EXAFS.[25] For the structure labeled I the distance between the Mn positions are 2.32, 1.71, 1.75, and 0.99 Å, respectively. The Ca positions differ by 2.10 Å. For structure II the corresponding distances are 1.88, 2.24, 1.03, 1.12, and for about 1.23 Å. For structure IIa they are 1.72, 2.15, 0.75, 1.44, and about 0.65 Å. Finally for structure III they are 1.82, 2.11, 1.01, 1.04, and about 1.13 Å. Overall the agreement with the DFT structure is worse than for the two X-ray structures. As noted before,[31] none of the proposed EXAFS models fit the anomalous diffraction map very well either.

The number of short Mn–Mn distances in the S_1 state has been a controversial issue with different suggestions. Metal–metal distances are known to be slightly too long using B3LYP, but the results are sufficiently accurate for a comparison to experiments when polarization functions have been used in the geometry optimization as in the present case. The Mn–Mn distances in the DFT S_1 structure are 2.74 Å (Mn3–Mn4), 2.81 Å (Mn1–Mn2), 2.87 Å (Mn1–Mn3), and 3.02 Å (Mn2–Mn3). Three rather short, and one longer distance is in basic agreement with one EXAFS interpretation,[25] even though the short ones are too long by 0.1 Å, and rather surprisingly, the long one is too short by a margin of nearly 0.3 Å, which could indicate that some amino acid is not at the correct position. Some of the deviations are probably due to the fact that Jahn–Teller distortions are somewhat exaggerated by DFT, see further below. The agreement is less good compared to another EXAFS study which suggests only two short distances.[26] For another DFT structure, with Mn4 reduced rather than Mn1 and which is only a few kcal mol^{-1} higher in energy, the distances are 2.81, 2.75, 2.80, and 3.04 Å. The second EXAFS study[26] actually suggests a protonation state with O_f protonated, which is a different charge state (a charge of -1 is discussed in a section below) than the one suggested here (charge -2). For that charge state, the energy of the O_f protonated state is only 3.2 kcal mol^{-1} higher than the lowest energy structure, and the Mn–Mn distances are 2.78, 2.99, 2.84, and 3.03 Å, in rather good agreement with those suggested in that EXAFS study. An argument against a structure where O_f is protonated, is that the deprotonation of this structure, where the proton eventually reaches Asp61 in the proton transfer chain, is rather complicated. The deprotonations of the presently suggested structures are much simpler see below).

One of the most interesting results of the present study is the overall remarkably good agreement between the optimized structure for the S_1 state with the one suggested in the second EXAFS study mentioned above.[26] The agreement includes a five-coordinated manganese in the Mn_3Ca

cube which is Mn2 in both cases. It also includes a short bond between Mn3 and the dangling manganese Mn4, connected by two μ-oxo bridges, of which one oxo group is removed from the cubic arrangement of Mn_3Ca. This agreement can be taken as support for both structures since they were obtained in entirely different ways. It is true that the Mn–Mn distances are not exactly the same but it is argued here that these differences are unlikely to have any significant direct impact on the mechanism for O–O bond formation.

The optimized S_1 structure is shown in Figure 8 with a different perspective to illustrate the hydrogen bonding of Arg357 and Ala344. Since Arg357 is positively charged it needs to be stabilized by several hydrogen bonds. It has been suggested from FTIR experiments that Ala344 does not bind to calcium,[27] and therefore could be a monodentate ligand to Mn1. A hydrogen bond between Ala344 and Arg357 therefore appears natural and was chosen in the model used here. At the same time this amino group of Arg357 forms an additional hydrogen bond to Oe. Since the other amino group of the guanidine side chain of Arg357 has problems reaching a good hydrogen bonding position, an additional water was placed in between O_b and the arginine. In the model used here, Ala344 forms an additional hydrogen bond to a water on calcium. Even though the present model is reasonably optimal, it is clear that other H-bonding alternatives are possible. At the very end of the present study, a bidentate bonding of Ala344 between Mn1 and calcium was investigated. This breaks the connection between Ala344 and Arg357 and actually fits the X-ray density slightly better.[32] The energies of that structure and the one in Figure 8 are nearly identical and the choice between these two structures should therefore not affect the mechanism very much.

The S-state transitions from start to end: With a resting S_1 state and with the procedure to obtain the other S states as described above, the entire mechanism from S_0 to dioxygen release in S_4 can now be summarized. The optimal S_0^{-2} state is shown schematically in Figure 9 and was formed from the S_1^{-2} state by adding an electron on Mn4 and a proton on O_b, which is bridging the dangling manganese and the Mn_3Ca cube. The oxidation states are then (III,III,IV,III). Since in S_3 all manganese are Mn^{IV}, this assignment of the S_0 state is in conflict with interpretations from FTIR, which suggest that the dangling manganese Mn4 is not oxidized in any S transition.[33] A large number of attempts to find a low-lying S_0 state with charge −1 or −2, which has Mn4 in oxidation state IV, all failed. However, it is not completely clear at the present stage that an oxidation of the dangling manganese must involve a frequency shift for Asp170, as assumed in the FTIR interpretations. To settle this question frequencies need to be calculated, which is under way, as well as calculations on larger models which could change the oxidation state of the dangling manganese to Mn^{IV}. The Mn–Mn distances of the S_0 structure in the Figure are 2.89, 2.86, 2.87, and 2.99 Å (in the same order as above).

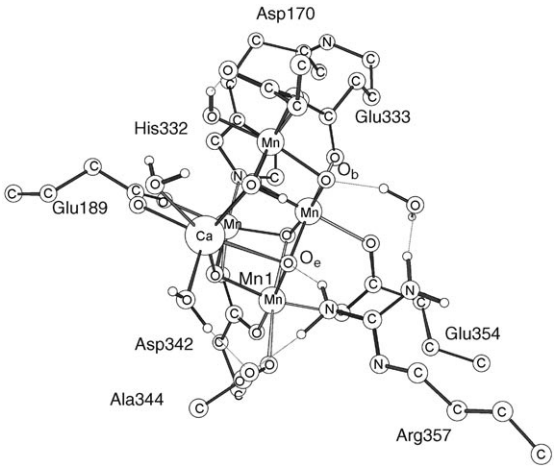

Figure 8. Different perspective of the S_1^{-2} state showing the hydrogen bonding of Arg357 and Ala344.

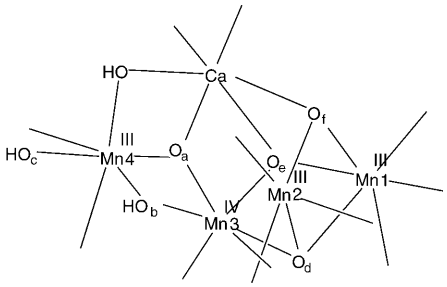

Figure 9. Simplified picture of the S_0^{-2} state.

The S_1^{-2} state has already been described above, but is shown again in schematic form in Figure 10. It is obtained from the S_0^{-2} state by oxidizing Mn4 and removing the proton on O_b leading to the oxidation states (III,III,IV,IV). The Mn–Mn distances in the Figure are 2.74, 2.81, 2.87, and 3.02 Å. Compared to the S_0 state, the most significant change occurs for the Mn3–Mn4 distance, which has changed by +0.15 Å, in good agreement with what has been suggested by EXAFS.[25,29] Removing the proton on O_b should be quite easy, since it is (via the external water, see Figure 8) in direct hydrogen bonding contact with Asp61 in the assumed proton transfer channel.

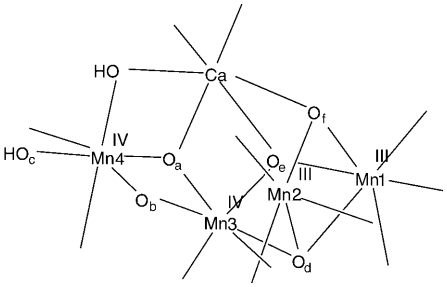

Figure 10. Simplified picture of the S_1^{-2} state.

The S_2^{-1} state is obtained from S_1^{-2} by removing an electron on Mn1. The oxidation states become (IV,III,IV,IV) and there does not seem to be a competitive candidate for this state. The S_2^{-1} state has a structure quite similar to the S_1^{-2} state. As discussed above, Mn2 is five-coordinated with the Jahn–Teller axis pointing towards the empty coordination site. The Mn–Mn distances are 2.70, 2.78, 2.75, and 3.15 Å (in the same order as above). The changes of the distances going from S_1 to S_2 are rather small but somewhat larger than suggested by EXAFS studies. One possible reason for this could be that DFT exaggerates changes due to Jahn–Teller distortions.[6] Another possibility is that S_1^{-2} actually should have oxidation states (IV,III,IV,III) instead. As mentioned above, this state is only a few kcal mol^{-1} higher in energy. With that S_1^{-2} state the change of Mn–Mn distances are very small in the transition going to S_2. However, an oxidation of the dangling manganese in this transition is not in line with FTIR experiments,[33] and the explanation for the discrepancy to EXAFS is therefore instead suggested to be a minor inaccuracy of DFT.

A very interesting aspect of the structures of the S_2^{-1} state and S_1^{-2} state, as shown in Figure 10, is that there are no protons left that could be easily removed. There are no protons on any of the oxo ligands, and the water derived ligand on Mn4 is a hydroxyl group that would form an unstable oxo group if it was deprotonated. This gives a very clear explanation for the experimental observation that only an electron, and no proton, leaves the OEC in the S_1 to S_2 transition.

The S_2 to S_3 transition is one of the most interesting steps in the dioxygen formation process. A significant structural reconstruction is implied by the EXAFS studies performed.[28,29] The reconstruction suggested by the present DFT calculations, already briefly described above, is shown in schematic form in Figure 11. An important general property of the type of mechanism suggested here is that protons and electrons leave in an alternating fashion from the OEC, in order not to build up charge unnecessarily. As mentioned above, the S_2^{-1} state is reached from the S_1^{-2} state by only removing an electron. At the next step a proton should therefore leave the OEC, but there are no easily removable protons in the S_2^{-1} state. One reason for the reconstruction in the S_2 to S_3 transition is therefore to add a water molecule from which a proton could be removed. However, the addition of a water with a simultaneous deprotonation is costly since Mn2 being Mn^{III} wants to remain five-coordinated. The resulting S_2^{-2} state is therefore quite unstable. By removing an electron from Mn2 in this S_2^{-2} state, reaching the S_3^{-1} state, stabilizes the OEC again since Mn^{IV} prefers to be six-coordinated. An additional complication of the addition of water is that it can not reach Mn2 but has to be added to Mn4, as shown in the figure.

The S_2 to S_3 transition can thus be summarized as described in the figure. A water molecule H_2O_g is first added to Mn4, forcing a loss of one of the other ligands (O_a) of this manganese. Instead, O_a forms a bond to Mn2 at its empty coordination site, making this Mn^{III} state six-coordinated. The water addition and the following deprotonation

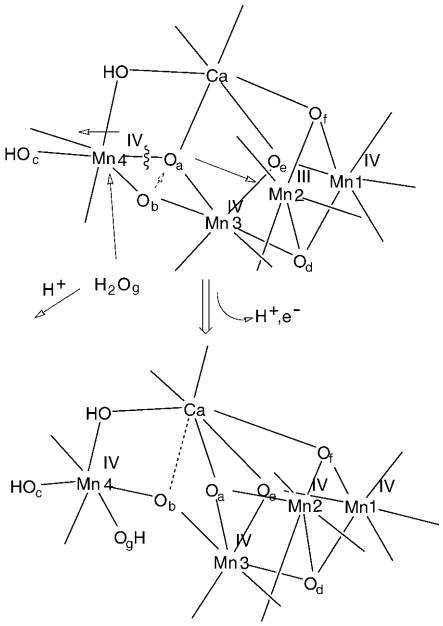

Figure 11. Structural rearrangement in the S_2^{-1} to S_3^{-1} transition.

of the water is an endergonic process leading to an unstable S_2^{-2} state. However, this state is stabilized by removing an electron from Mn2 making it Mn^{IV}, which prefers to be six-coordinated, reaching the S_3^{-1} state. The most important aspect of this reconstruction is that it leads to an increase of the distance between Mn4 and the Mn_3Ca cube that is necessary for the O–O bond formation, see below. Finally, the proton removed from O_g in the S_2 to S_3 transition can rather easily reach Asp61 in the proton transfer channel via the hydroxyl ligand OH_c, Asp170 and the external water.

In the preceding section it was shown that for the S_2 state, the present compact structure in Figure 11 is more favorable energetically than the more open type of structure shown for the S_4 state in Figure 3. It is also possible to ask the reverse question whether a more compact structure would also be energetically preferable for S_3. It is not possible to answer this question for the present complexes with a charge of −1, since a proton has to be removed directly after adding a water to S_2, and before the electron can be removed to reach S_3. However, for a complex of charge 0 a comparison can be made. For this charge state, the calculations indeed give a preference for the open structure of S_3 with a margin of 5.0 kcal mol^{-1}. In other words, adding a water to the S_2 state and opening up the structure gives an additional driving force for the S_2 to S_3 transition of 5.0 kcal mol^{-1}.

Since in S_3 all manganese atoms have oxidation state Mn^{IV}, an oxygen radical (O_g(rad)) is formed in the S_3 to S_4 transition, as shown in Figure 12 by removing both a proton and an electron. As mentioned in the introduction, an oxygen radical has been an important part of all O–O bond formation mechanisms suggested so far by the DFT calculations.[4–16] This process has furthermore always been found to be endergonic and will therefore contribute to the rate-

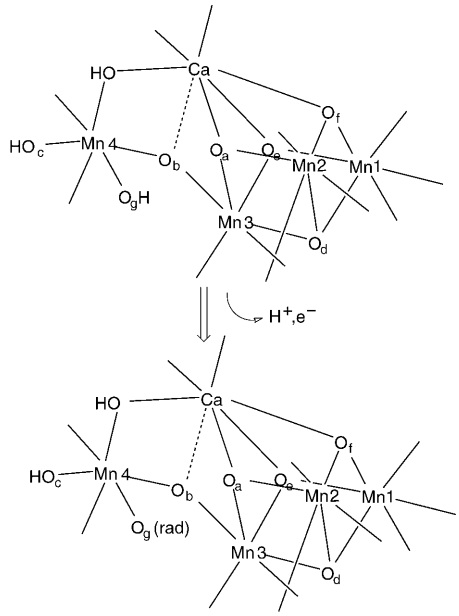

Figure 12. Simplified picture of the S_3^{-1} to S_4^{-1} transition.

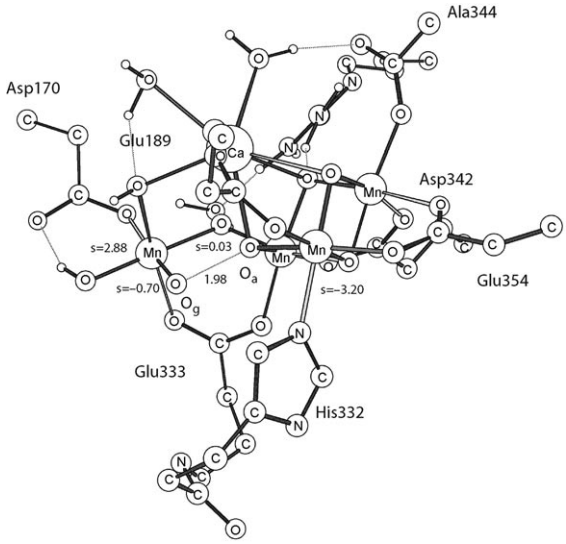

Figure 13. Transition state for O–O bond formation in the S_4^{-1} state. Most of the amino acid protons have been removed for a better visualization.

limiting barrier for O–O bond formation, see further below. The spin on oxygen is −0.89, coupled antiferromagnetically to the spin of the dangling manganese. The proton removed from O_g in the S_3 to S_4 transition can reach Asp61 in the same way as in the S_2 to S_3 transition.

By removing the protons and electrons in the earlier S transitions, as described above, and making the structural reconstruction in the S_2 to S_3 transition, the complex is now optimally set up to form the O–O bond between the oxygen radical (O_g(rad)) and the oxo group (O_a). The electronic structure requirements for a low barrier has been described recently in several reviews[15,16] and will not be repeated in detail. The spins have to be alternating (+−+−) for the four atoms directly involved, Mn4, O_g, O_a, and Mn2, for a low barrier.[14] The optimized transition state is shown in Figure 13. The computed B3LYP* barrier for this step is 6.5 kcal mol^{-1}, which includes a contribution of a spin-correction lowering the reactant by 2.6 kcal mol^{-1}. It should be remembered that the rate-limiting barrier for O–O bond formation also includes the endergonic transition to reach the S_4^{-1} state. To obtain the energy for that transition, relative pK_a values and redox potentials for the complete catalytic cycle is involved, which will be discussed in the next section.

For completeness, the leading alternative mechanism for O–O bond formation was also computed. In this mechanism the oxygen radical reacts with an external water molecule rather than with an oxo group. This mechanism was originally suggested from DFT studies on simpler models[4,5] but has been suggested recently again based on QM/MM studies.[17] The computed barrier for this mechanism using the present model is 28.1 kcal mol^{-1} using B3LYP and lacvp geometries. At the same level, the barrier for the mechanism described above is 6.8 kcal mol^{-1}.

The final step in the S-state cycle is to exchange dioxygen with a water molecule. This is a complicated process and has not yet been studied in detail. Only the thermodynamics of this step is needed in the energy diagram described below. The product of the exchange is an S_0^{-1} state which was found from the best S_0^{-2} state in Figure 9, by adding a proton on HO_c.

Energy diagrams

In the calculations discussed above, relative pK_a values and redox potentials have been computed for all S states. These values can be put on an absolute scale by a procedure described in other papers.[7–13] First, the driving force for the full catalytic cycle is taken from experimental redox potentials. From the redox potential for P_{680} of 1.3 V and for water of 0.8 V, the driving force becomes 46 kcal mol^{-1}, and this was the value used in most previous studies.[15] However, the present diagrams differ somewhat on this point. In the present case, the experimental observation[34,35] that the Tyr_Z radical is formed after electron transfer to $P^{+,680}$, indicating that it should be at least 3 kcal mol^{-1} more stable than $P^{+,680}$, is incorporated into the diagrams. It is assumed that the loss of energy is as small as possible not to waste energy unnecessarily. This reduces the total driving force by $4\times3=12$ kcal mol^{-1} from 46 to 34 kcal mol^{-1}. To construct the full energy diagram an additional, adjustable, parameter has to be used, which is chosen to make the barriers as small as possible and to make (if possible) the S-state transitions exergonic.

In the S-state transitions discussed above, the OEC alternates between a charge of −2 and −1. This decision was actually one of the most difficult ones to make based on the present calculations. Alternating charges between −1 and 0 is also a possibility, and was chosen in most of the earlier

studies. There are a few reasons for making the present choice. One reason is that this choice gives a very natural explanation for why only an electron, and no proton, is transferred in the S_1 to S_2 transition, as described above. Another reason is that this choice gave a ground state for S_1 with the dangling manganese in oxidation state IV in line with FTIR experiments,[33] which the other choice did not. However, the main reason for the present choice was that in preliminary calculations with a larger model including Asp61, there was a strong tendency for the OEC to lose a proton artificially to Asp61 if the cluster had a charge of zero, which did not happen for more negative clusters. Still, in the present section both choices of alternating charges will be described.

The energy diagram for the case when the charge of the OEC alternates between −1 and −2 is shown in Figure 14. The general shape of the diagram is the same as in earlier studies.[15,16] The first two S-state transitions are energetically easy with a relatively large loss of energy, while the third one is much harder. From S_3 there is first an endergonic transition to S_4 of 11.9 kcal mol^{-1} followed by the step where the O–O bond is formed with a barrier of 6.5 kcal mol^{-1}. Altogether, from S_3 there is thus a barrier of $(11.9+6.5)=18.4$ kcal mol^{-1}, which is somewhat larger than the barrier of 13–14 kcal mol^{-1} estimated from transition state theory for a process requiring milliseconds. A too high barrier is common for B3LYP (and B3LYP*). For example, it is difficult to get a perfect balance between the redox potential of manganese and oxygen. If the former one is artificially favored by DFT, the barrier will be too high. In this context it should be remembered that the leading alternative mechanism, a reaction with an external water, has a barrier more than 20 kcal mol^{-1} higher, that is, higher than 38 kcal mol^{-1} with the present model.

One of the most interesting aspects of the energy diagram in Figure 14 is the very small driving force of 3.7 kcal mol^{-1} from S_3 to S_0. This is different from the earlier study based on the ligand orientations of the Berlin X-ray structure, where a driving force of 13.4 kcal mol^{-1} was found for this transition. The reasons for this difference are that a larger total driving force was used, that B3LYP* was used rather than B3LYP, that Arg357 was included in the model, and that the present models more closely follow the X-ray structure by fixing certain coordinates. An interesting conclusion which can be drawn from the small driving force obtained, is that the process is reversible. This has implications for interpreting water exchange experiments,[36] for which both oxygens were found to be exchangeable, one very quickly and one rather slowly. An argument against involvement of an oxo ligand in the formation of the O–O bond is that for model complexes it appears that exchange of oxo ligands with water is normally much too slow to match the water exchange rates measured for the OEC.[37] However, if O–O bond formation is reversible, the following set of events could explain how both oxygens of O_2 could exchange with water. One of the oxygens making O_2 could first exchange at the easily exchanging site. The O_2 product could then reversibly go back, cleave its bond, and position the oxygen that has not been exchanged at the easily exchanging site, and make the O–O bond again by going forwards to S_0. This would imply that the slow exchange should have a barrier which is higher than the one for fast exchange by the exergonicity in the S_3 to S_0 transition, that is, in this case by 3.7 kcal mol^{-1}. The measurements indicate a barrier difference of 2–3 kcal mol^{-1},[36] in reasonable agreement with the present estimate. This channel for oxygen exchange is only open for metal complexes which can form dioxygen in a process which is reversible, and does therefore not apply to any known metal complexes except the OEC. However, it should be added that the present mechanism can hardly explain the quite different exchange rates in S_0 and S_1. In S_0 there should instead be a pathway for direct exchange between a bridging oxo (or hydroxo) and water. Investigations of this type of pathway is in progress.

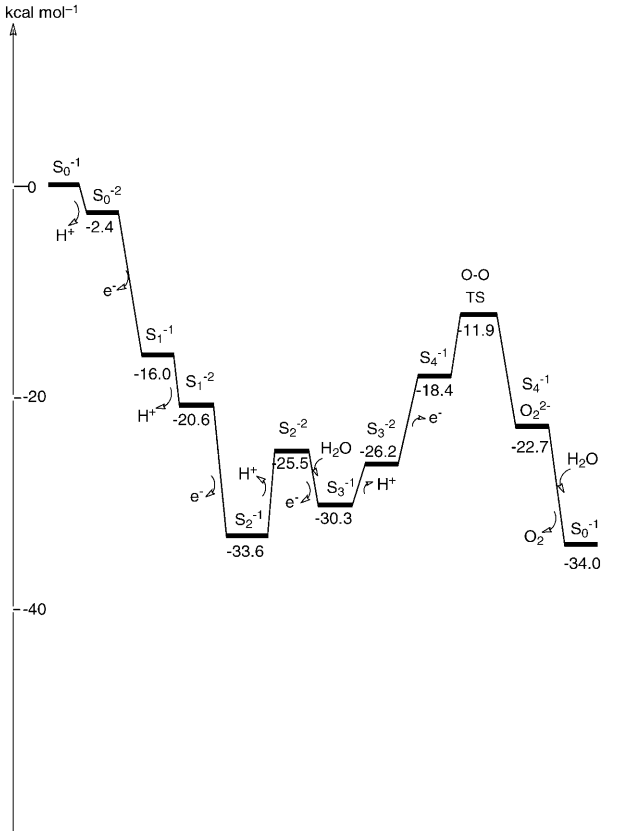

Figure 14. Energy diagram for dioxygen formation in PSII. The charge of the OEC alternates between −1 and −2.

Reversibility of the final step(s) of dioxygen formation has been implied by experiments in which the oxygen pressure was varied.[38] When the pressure increased, an equilibrium was observed between free dioxygen and another state. From the energy diagram in Figure 14, this state is here suggested to be one where the O–O bond is cleaved, probably in the S_3 state. A peroxide state is much less likely since it is 11.3 kcal mol^{-1} higher than free dioxygen in the diagram.

In the present mechanism, water is inserted into the OEC at two different occasions, see Figure 14. The first time is in the S_2 to S_3 transition (in the literature this water is sometimes called the second water). At this point binding of a water molecule is needed since there are no easily removable protons left on the OEC in the S_2^{-1} state. The addition of this water is of critical importance for the mechanism since the OEC opens up in this process, which is necessary for the O–O bond formation step. The second water enters in the S_4 to S_0 transition, and replaces dioxygen when it is expelled from the OEC. The two points where water binds to the OEC is in good agreement with interpretations of recent FTIR measurements,[39] although it is concluded in that paper that water may not bind directly to the metals in these transitions. The present suggestion is also in line with interpretations of a recent ^{17}O-HYSCORE spectroscopic measurement, where only one substrate water was suggested to be bound in S_2.[40] However, it does not fully agree with interpretations based on membrane-inlet mass spectrometry measurements,[41] where both substrate waters were suggested to be bound in the S_2 state, but it is not clear whether these waters should both be directly bound to the cluster or just hydrogen-bonding to ligands of the cluster. Also, the kinetics for the fast exchange in S_2 is very close to the time resolution of that method.

While many aspects of the energy diagram agree with observations, there are also a few remaining discrepancies. One has already been mentioned and concerns the too high rate limiting barrier. Another one is that the S_2 state is lower than the S_3 state. These errors are not possible to correct by another choice of the adjustable parameter. Since the errors are rather small it is quite possible that these problems are due to inaccuracies of the DFT method and cannot be corrected without going to a more accurate method. It is also possible that the errors are due to limitations or some other inadequacy of the present model. A natural extension of the model is to include Asp61 which is the second nearby charged residue, apart from Arg357. Such calculations are in progress. Another inadequacy of the model could be the rather uncertain position of Asp170, which has been given two quite different positions in the two X-ray structures. A position further out than in the London structure, which is used here, more like the one suggested in the Berlin structure, could stabilize the more open structures. This would lower the energy of S_3 compared to S_2, and perhaps put the former state lower in energy.

The energy diagram obtained when the charge alternates between 0 and −1 is shown in Figure 15. The states in this diagram are basically the same as in the earlier diagram with the difference that there is an additional proton on the HO_c ligand on the dangling manganese. The first comment that can be made about the diagram in Figure 15 is that it is very similar to the one in Figure 14. Important similarities include the overall shape, the mechanism for O–O bond formation, and the small driving force for the S_3 to S_0 transition. There are also some minor differences. The rate-limiting barrier from S_3 for the second diagram is (31.4–15.5) = 15.9 kcal mol^{-1}, which is 2.5 kcal mol^{-1} lower than the one in the first diagram. The S_2 state is also in the second diagram lower than the S_3 state, but only by 0.6 kcal mol^{-1}. Both these differences favor the second diagram. However, that diagram does not explain why only an electron, and no proton, is transferred in the S_1 to S_2 transition. On the contrary, if the diagram is strictly followed it actually suggests that two protons leave in this transition. It should be remembered that this happens with only a very small energetic margin, and can not be used to rule out this diagram, since the error could well be due to a minor inaccuracy of the DFT method used. The differences between the diagrams for this transition can be explained by the presence of the additional proton. This means that when the S_2^0 state is reached, there is this additional proton which can relatively easily be removed, going to the S_2^{-1} state. This possibility does not exist for the other diagram. In summary, future calculations are required to sort out the remaining discrepancies. In the meantime, similarities and differences between the diagrams can be used to draw conclusions concerning what is safely predicted and what remains uncertain.

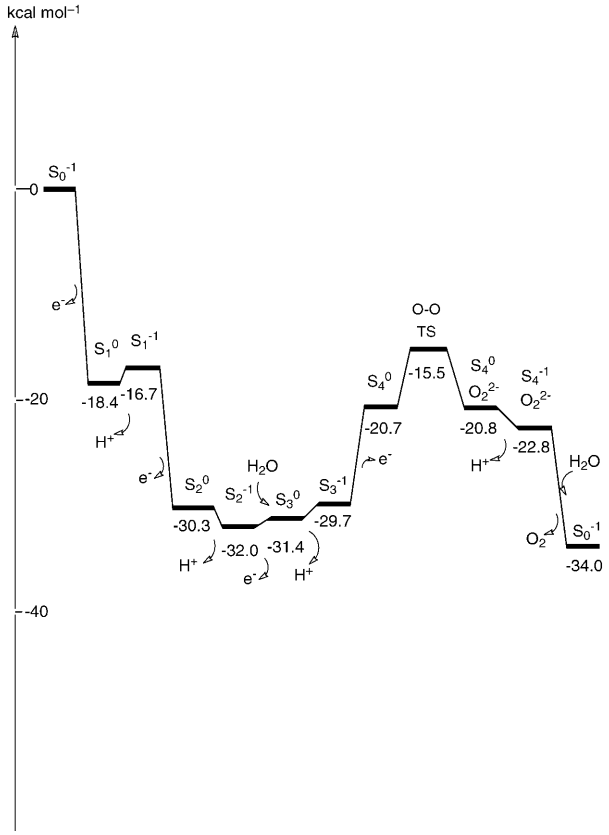

Figure 15. Energy diagram for dioxygen formation in PSII. The charge of the OEC alternates between 0 and −1.

Conclusions

In the present study, the O–O bond formation mechanism suggested previously[14] has been used as a starting point for obtaining structures and energies for all the S states. In order to stay as closely as possible to the X-ray structures, the positions of the backbone atoms included in the model were held fixed at the positions suggested by the London structure.[1] The ligation pattern was taken from the Berlin structure.[2] The following main structural results were obtained. First, the optimized structure for the S_1 state quite strongly resembles the one suggested in a recent EXAFS study.[26] Most of all, there is a short Mn–Mn bond length between the dangling manganese and the Mn_3Ca cube, and Mn2 in the cube is only five-coordinated. The number of short Mn–Mn bonds is three, more in line with another EXAFS study.[25] Second, a reconstruction of the OEC is found in the S_2 to S_3 transition also in agreement with suggestions from EXAFS.[28,29] This reconstruction is caused by a binding of a water molecule which opens up the OEC from the rather compact structure found for the lower S states. This leads to an increase of the distance between the dangling manganese and the cube, which is necessary for an optimal O–O bond formation in the S_4 state. The Mn-oxidation states derived for the S_0, S_1 and S_2 states and structural change in the S_0 to S_1 transition are very similar to those derived in a recent ^{55}Mn ENDOR study.[42] There is also agreement on the structural changes reported by EXAFS.[29,43]

The first water molecule binds to the OEC in the S_2 to S_3 transition causing the reconstruction. The second one replaces the dioxygen molecule when it is expelled in the S_4 to S_0 transition. These results are in agreement with recent FTIR,[39] and ^{17}O-HYSCORE spectroscopic measurements, but in slight disagreement with membrane-inlet mass spectrometry measurements.[41] The protons and electrons leave the OEC in an alternating fashion, with one proton leaving in each transition except in S_1 to S_2 where only an electron leaves. The reason for this is that there are no easily removable protons left on the OEC at that stage. All μ-oxo bridges are already deprotonated and the only water derived ligand is a terminal hydroxyl group. All four protons removed can rather easily move to Asp61 in the suggested proton transfer channel. One of them is connected directly to Asp61 over one water molecule. The other three protons move via a terminal hydroxyl group and Asp170 over to Asp61.

The mechanism for O–O bond formation is the same as suggested in earlier studies. An oxygen radical held by the dangling manganese reacts with an oxo ligand in the Mn_3Ca cube. From the computed energy diagram the barrier counted from S_3 is 18.4 kcal mol^{-1}, which is a few kcal mol^{-1} higher than the experimental value of 13–14 kcal mol^{-1}. The endergonic transition from S_3 to S_4 is included in the barrier. The leading alternative to this mechanism is one where the oxygen radical reacts with an external water, which was found to have a barrier close to 40 kcal mol^{-1}.

An interesting result, observed in the energy diagram, is that O–O bond formation appears reversible. This leads to a possibility for water exchange not considered earlier. Both oxygen atoms would then use the fast exchanging site, but the slowly exchanging oxygen has to use the reversibility of O–O bond formation to go back to S_3, by cleaving the O–O bond, and then use the fast exchanging site once more. The present energy diagram suggests that the barrier for the slow exchange should be about 4 kcal mol^{-1} higher than the one for the fast exchange, in reasonable agreement with the experimental value of 2–3 kcal mol^{-1}.[36]

While there are many results that agree with experimental observations, there are also a few minor remaining discrepancies. The most striking one of these is that the energy of S_2 was found to be lower than the one of S_3. Since the error is small it could be due to limitations of the accuracy of B3LYP. Other possibilities involving limitations of the models used will be investigated in the future. An interesting possibility is that the present positioning of Asp170 is not correct. A place further out from the cube should lead to results in the right direction.

Acknowledgement

I am very grateful to James Barber and James Murray for many discussions and J.M. for preparing Figure 4 of the present paper.

[1] K. N. Ferreira, T. M. Iverson, K. Maghlaoui, J. Barber, S. Iwata, *Science* **2004**, *303*, 1831–1838.
[2] B. Loll, J. Kern, W. Saenger, A. Zouni, J. Biesiadka, *Nature* **2005**, *438*, 1040–1044.
[3] V. K. Yachandra, K. Sauer, M. P. Klein, *Chem. Rev.* **1996**, *96*, 2927–2950.
[4] P. E. M. Siegbahn, R. H. Crabtree, *J. Am. Chem. Soc.* **1999**, *121*, 117–127.
[5] P. E. M. Siegbahn, *Inorg. Chem.* **2000**, *39*, 2923–2935.
[6] M. Lundberg, P. E. M. Siegbahn, *Phys. Chem. Chem. Phys.* **2004**, *6*, 4772–4780.
[7] P. E. M. Siegbahn, M. Lundberg, *Photochem. Photobiol. Sci.* **2005**, *4*, 1035–1043.
[8] P. E. M. Siegbahn, M. Lundberg, *J. Inorg. Biochem.* **2006**, *100*, 1035–1040.
[9] P. E. M. Siegbahn, *Adv. Inorg. Chem.* **2004**, *56*, 101–125; P. E. M. Siegbahn, J. W. Tye, M. B. Hall, *Chem. Rev.* **2007**, *107*, 4414–4435.
[10] P. E. M. Siegbahn, M. R. A. Blomberg, *J. Phys. Chem. B* **2003**, *107*, 10946–10955; M. R. A. Blomberg, P. E. M. Siegbahn, *J. Comput. Chem.* **2006**, *27*, 1373–1384.
[11] L. M. Blomberg, M. R. A. Blomberg, P. E. M. Siegbahn, *Biochim. Biophys. Acta Bioenerg.* **2006**, *1757*, 31–46; L. M. Blomberg, M. R. A. Blomberg, P. E. M. Siegbahn, *Biochim. Biophys. Acta Bioenerg.* **2006**, *1757*, 240–252; L. M. Blomberg, M. R. A. Blomberg, P. E. M. Siegbahn, *J. Biol. Inorg. Chem.* **2007**, *12*, 79–89.
[12] P. E. M. Siegbahn, A. F. Shestakov, *J. Comput. Chem.* **2005**, *26*, 888–898.
[13] P. E. M. Siegbahn, M. R. A. Blomberg, in *Computational Modeling for Homogeneous Catalysis and Biocatalysis* (Eds.: K. Morokuma, J. Musaev), Wiley-VCH, Germany, **2008**, p. 57–81.
[14] P. E. M. Siegbahn, *Chem. Eur. J.* **2006**, *12*, 9217–9227.
[15] P. E. M. Siegbahn, *Phil. Trans. R. Soc. B* **2008**, *363*, 1221–1228.
[16] P. E. M. Siegbahn, *Inorg. Chem.* **2008**, *47*, 1779–1786.
[17] E. M. Sproviero, J. A. Gascon, J. P. McEvoy, G. W. Brudvig, V. S. Batista, *J. Chem. Theory Comput.* **2006**, *4*, 1119–1134; E. M. Sproviero,

J. A. Gascon, J. P. McEvoy, G. W. Brudvig, V. S. Batista, *Curr. Op. Struct. Biol.* **2007**, *17*, 173–180; E. M. Sproviero, K. Shinopoulos, J. A. Gascon, J. P. McEvoy, G. W. Brudvig, V. S. Batista, *Phil. Trans. R. Soc. B* **2008**, *363* 1149–1156.
[18] J. S. Vrettos, D. A. Stone, G. W. Brudvig, *Biochemistry* **2001**, *40*, 7937–7945; corrections: J. S. Vrettos, D. A. Stone, G. W. Brudvig, *Biochemistry* **2003**, *42*, 848.
[19] A. D. Becke, *J. Chem. Phys.* **1993**, *98*, 5648–5652.
[20] P. E. M. Siegbahn, *J. Biol. Inorg. Chem.* **2006**, *11*, 695–701.
[21] L. Noodleman, D. A. Case, *Adv. Inorg. Chem.* **1992**, *38*, 423–470.
[22] M. Reiher, O. Salomon, B. A. Hess, *Theor. Chem. Acc.* **2001**, *107*, 48–55.
[23] Jaguar 5.5, L. L. C. Schrödinger, Portland, OR, **1991–2003**.
[24] Gaussian 03 (Revision B.03), M. J. Frisch, G. W. Trucks, H. B. Schlegel, G. E. Scuseria, M. A. Robb, J. R. Cheeseman, J. A. Montgomery, Jr., T. Vreven, K. N. Kudin, J. C. Burant, J. M. Millam, S. S. Iyengar, J. Tomasi, V. Barone, B. Mennucci, M. Cossi, G. Scalmani, N. Rega, G. A. Petersson, H. Nakatsuji, M. Hada, M. Ehara, K. Toyota, R. Fukuda, J. Hasegawa, M. Ishida, T. Nakajima, Y. Honda, O. Kitao, H. Nakai, M. Klene, X. Li, J. E. Knox, H. P. Hratchian, J. B. Cross, V. Bakken, C. Adamo, J. Jaramillo, R. Gomperts, R. E. Stratmann, O. Yazyev, A. J. Austin, R. Cammi, C. Pomelli, J. W. Ochterski, P. Y. Ayala, K. Morokuma, G. A. Voth, P. Salvador, J. J. Dannenberg, V. G. Zakrzewski, S. Dapprich, A. D. Daniels, M. C. Strain, O. Farkas, D. K. Malick, A. D. Rabuck, K. Raghavachari, J. B. Foresman, J. V. Ortiz, Q. Cui, A. G. Baboul, S. Clifford, J. Cioslowski, B. B. Stefanov, G. Liu, A. Liashenko, P. Piskorz, I. Komaromi, R. L. Martin, D. J. Fox, T. Keith, M. A. Al-Laham, C. Y. Peng, A. Nanayakkara, M. Challacombe, P. M. W. Gill, B. Johnson, W. Chen, M. W. Wong, C. Gonzalez, J. A. Pople, Gaussian, Inc., Wallingford CT, **2003**.
[25] J. Yano, J. Kern, K. Sauer, M. J. Latimer, Y. Pushkar, J. Biesiadka, B. Loll, W. Saenger, J. Messinger, A. Zouni, V. K. Yachandra, *Science* **2006**, *314*, 821–825; J. Yano, J. Kern, Y. Pushkar, K. Sauer, P. Glatzel, U. Bergmann, J. Messinger, A. Zouni, V. K. Yachandra, *Phil. Trans. R. Soc. B* **2008**, *363* 1139–1147.
[26] H. Dau, A. Grundmeier, P. Loja, M. Haumann, *Phil. Trans. R. Soc. B* **2008**, *363* 1237–1244.
[27] M. A. Strickler, L. M. Walker, W. Hillier, R. J. Debus, *Biochemistry* **2005**, *44*, 8571–8577.
[28] W. Liang, T. A. Roelofs, R. M. Cinco, A. Rompel, M. J. Latimer, W. O. Yu, K. Sauer, M. P. Klein, V. K. Yachandra, *J. Am. Chem. Soc.* **2000**, *122*, 3399–3412.
[29] M. Haumann, C. Muller, P. Liebisch, L. Iuzzolino, J. Dittmer, M. Grabolle, T. Neisius, W. Meyer-Klaucke, H. Dau, *Biochemistry* **2005**, *44*, 1894–1908.
[30] J. Yano, J. Kern, K.-D. Irrgang, M. J. Latimer, U. Bergmann, Y. Glatzel, P. Pushkar, J. Biesiadka, B. Loll, K. Sauer, J. Messinger, A. Zouni, V. K. Yachandra, *Proc. Natl. Acad. Sci. USA* **2005**, *102*, 12047–12052.
[31] J. Barber, J. W. Murray, *Phil. Trans. R. Soc. B* **2008**, *363*, 1129–1138.
[32] J. Murray, private communication, **2007**.
[33] R. J. Debus, M. A. Strickler, L. M. Walker, W. Hillier, *Biochemistry* **2005**, ***44***, 1367–1373.
[34] K. Brettel, E. Schlodder, H. T. Witt, *Biochim. Biophys. Acta Bioenerg.* **1984**, *766*, 403–415.
[35] G. Renger, *Biochim. Biophys. Acta Bioenerg.* **2004**, *1655*, 195–204.
[36] W. Hillier, J. Messinger, *Adv. Photosynth. Respir.* **2005**, *22*, 567–608.
[37] G. W. Brudvig, *Phil. Trans. R. Soc. B* **2008**, *363* 1211–1219.
[38] J. Clausen, W. Junge, *Nature* **2004**, *430*, 480–483.
[39] T. Noguchi, *Phil. Trans. R. Soc. B* **2008**, *363*, 1189–1195.
[40] J.-H. Su, W. Lubitz, J. Messinger, *J. Am. Chem. Soc.* **2008**, *130*, 786–787.
[41] G. Hendry, T. Wydrzynski, *Biochemistry* **2002**, *41*, 13328–13334.
[42] L. Kulik, B. Epel, W. Lubitz, J. Messinger, *J. Am. Chem. Soc.* **2007**, *129*, 13421–13435.
[43] J. H. Roblee, J. Messinger, R. M. Cinco, K. L. McFarlane, C. Fernandez, S. A. Pizarro, K. Sauer, V. K. Yachandra, *J. Am. Chem. Soc.* **2002**, *124*, 7459–7471.

Received: March 11, 2008
Published online: August 4, 2008

